

Overactive bladder mediated by accelerated Ca^{2+} influx mode of $\text{Na}^+/\text{Ca}^{2+}$ exchanger in smooth muscle

Hisao Yamamura,^{1*} William C. Cole,^{2*} Satomi Kita,³ Shingo Hotta,¹ Hidemichi Murata,¹ Yoshiaki Suzuki,¹ Susumu Ohya,^{1,4} Takahiro Iwamoto,³ and Yuji Imaizumi¹

¹Department of Molecular and Cellular Pharmacology, Graduate School of Pharmaceutical Sciences, Nagoya City University, Nagoya, Japan; ²The Smooth Muscle Research Group, Department of Physiology and Pharmacology, Faculty of Medicine, University of Calgary, Calgary, Canada; ³Department of Pharmacology, Faculty of Medicine, Fukuoka University, Fukuoka, Japan; and ⁴Department of Pharmacology, Division of Pathological Sciences, Kyoto Pharmaceutical University, Kyoto, Japan

Submitted 4 March 2013; accepted in final form 13 May 2013

Yamamura H, Cole WC, Kita S, Hotta S, Murata H, Suzuki Y, Ohya S, Iwamoto T, Imaizumi Y. Overactive bladder mediated by accelerated Ca^{2+} influx mode of $\text{Na}^+/\text{Ca}^{2+}$ exchanger in smooth muscle. *Am J Physiol Cell Physiol* 305: C299–C308, 2013. First published May 22, 2013; doi:10.1152/ajpcell.00065.2013.—The $\text{Na}^+/\text{Ca}^{2+}$ exchanger (NCX) is thought to be a key molecule in the regulation of cytosolic Ca^{2+} dynamics. The relative importance of the two Ca^{2+} transport modes of NCX activity leading to Ca^{2+} efflux (forward) and influx (reverse) in smooth muscle, however, remains unclear. Unexpectedly, spontaneous contractions of urinary bladder smooth muscle (UBSM) were enhanced in transgenic mice overexpressing NCX1.3 (NCX1.3^{tg/tg}). The enhanced activity was attenuated by KB-R7943 or SN-6. Whole cell outward NCX current sensitive to KB-R7943 or Ni^{2+} was readily detected in UBSM cells from NCX1.3^{tg/tg} but not wild-type mice. Spontaneous Ca^{2+} transients in myocytes of NCX1.3^{tg/tg} were larger and frequently resulted in propagating events and global elevations in cytosolic Ca^{2+} concentration. Significantly, NCX1.3^{tg/tg} mice exhibited a pattern of more frequent urination of smaller volumes and this phenotype was reversed by oral administration of KB-R7943. On the other hand, KB-R7943 did not improve it in KB-R7943-insensitive (G833C-) NCX1.3^{tg/tg} mice. We conclude that NCX1.3 overexpression is associated with abnormal urination owing to enhanced Ca^{2+} influx via reverse mode NCX leading to prolonged, propagating spontaneous Ca^{2+} release events and a potentiation of spontaneous UBSM contraction. These findings suggest the possibility that NCX is a candidate molecular target for overactive bladder therapy.

sodium/calcium exchanger; urinary bladder; smooth muscle; overactive bladder; KB-R7943

$\text{Na}^+/\text{Ca}^{2+}$ EXCHANGERS (NCXs) are expressed in a variety of cell types and participate in the regulation of cytosolic Ca^{2+} mobilization. For example, the physiological and pathological roles of NCX are well understood in cardiac myocytes (6, 41). NCX is a bidirectional antiporter that transports three Na^+ per Ca^{2+} ion in an electrogenic manner. Normally, the large inwardly directed electrochemical gradient for Na^+ results in forward mode NCX activity and Ca^{2+} efflux to maintain Ca^{2+} homeostasis following influx through voltage-dependent Ca^{2+} channels (VDCCs) and Ca^{2+} -induced Ca^{2+} release (CICR)

from internal stores during excitation-contraction coupling (4). Genetic deletion of NCX (i.e., NCX1-deficient mice, NCX1^{-/-}) is an embryonically lethal knockout, presumably because of abnormal Ca^{2+} homeostasis and associated cardiac development and dysfunction (45). Whether reverse mode NCX activity is associated with Na^+ accumulation in the subplasmalemmal space during the cardiac action potential to provide additional trigger Ca^{2+} influx remains controversial (33). However, it is well-established that elevated cytosolic Na^+ concentration ($[\text{Na}^+]_i$) owing to decreased intracellular pH and increased Na^+/H^+ exchange activity, combined with membrane potential depolarization in cardiac ischemia/reperfusion injury provides an appropriate electrogenic environment for enhanced Ca^{2+} influx via reverse mode NCX leading to Ca^{2+} overload and associated electrical and mechanical dysfunction (arrhythmias; Refs. 4, 6, 41). Moreover, suppression of NCX activity with KB-R7943, a benzylphenyl NCX inhibitor, or heterozygous deletion improves ischemia/reperfusion-induced dysfunction in the heart (28) and kidney (52).

In contrast, the physiological role(s) of NCX in smooth muscle appears to be more complicated, as forward and reverse modes have both been postulated to be functionally relevant in controlling cytosolic Ca^{2+} dynamics in different preparations (3, 9, 40). In mammals, three NCX isoforms have been identified as products of the SLC8 gene family (37). NCX1 is abundant in the heart and brain and also expressed at much lower levels in other tissues, whereas the expression of NCX2 and NCX3 is restricted mainly to brain and skeletal muscle. Among alternative splicing variants of NCX1, NCX1.3 and NCX1.7 are the predominant isoforms expressed in smooth muscle tissues (38). NCX1 was suggested to contribute to Ca^{2+} extrusion when cytosolic Ca^{2+} concentration ($[\text{Ca}^{2+}]_i$) is suddenly elevated (9, 42, 51). For example, we previously reported that Ca^{2+} extrusion was enhanced after stimulation in urinary bladder smooth muscle (UBSM) of transgenic mice specifically overexpressing NCX1.3 in smooth muscles (NCX1.3^{tg/tg}), whereas increased reverse mode activity was evident when the transmembrane Na^+ gradient was reduced by reduction of extracellular $[\text{Na}^+]$ ($[\text{Na}^+]_o$; Ref. 32). Significantly, reverse mode NCX activity was shown to predominate under resting conditions in vascular smooth muscle of NCX1.3^{tg/tg} mice leading to elevated systemic blood pressure and salt-sensitive hypertension, whereas a selective NCX inhibitor, SEA0400, was found to lower blood pressure in salt-dependent hypertensive animal models (23). Moreover, upregulation of NCX and enhanced function in the reverse mode were also previously

* H. Yamamura and W. C. Cole contributed equally to this study as major investigators.

Address for reprint requests and other correspondence: Y. Imaizumi, Dept. of Molecular and Cellular Pharmacology, Graduate School of Pharmaceutical Sciences, Nagoya City Univ. 3-1 Tanabedori, Mizuhoku, Nagoya 467-8603, Japan (e-mail: yimaizum@phar.nagoya-cu.ac.jp).

reported to be associated with ouabain-induced hypertension (36) and pulmonary arterial hypertension (55).

In preliminary experiments, we unexpectedly found that spontaneous contractions of UBSM were enhanced in NCX1.3^{tg/tg} compared with wild-type (WT) mice. For this reason, the present study was undertaken to elucidate the contribution of Ca²⁺ influx via reverse mode NCX activity to the control of membrane electrical excitability, cytosolic Ca²⁺ mobilization in UBSM myocytes, UBSM contractility, and urinary bladder function.

MATERIALS AND METHODS

Experimental animals. All experiments were approved by the Ethics Committee of the Nagoya City University and were conducted in accordance with the *Guide for the Care and Use of Laboratory Animals* of the Japanese Pharmacological Society. The generations of the NCX1.3^{tg/tg} and G833C-NCX1.3^{tg/tg} mice were described previously (22, 23). Data from NCX1.3^{tg/tg} and G833C-NCX1.3^{tg/tg} mice were compared with age-matched WT mice (C57BL/6; Japan SLC, Hamamatsu, Japan).

Contractility measurements. Measurements of UBSM contractility were carried out as reported previously (31). In brief, urinary bladders were removed from male mice (8–12 wk old) and placed in aerated Krebs solution. A small strip (1 mm in wide and 5 mm in long) of detrusor muscle was prepared and placed in a tissue bath containing aerated Krebs solution at 37°C. One end of the segment was pinned to a rubber plate at the bottom of the bath, and the other end was connected to an isometric transducer. Strips were stretched to ~1 mN of tension. The Krebs solution had an ionic composition of 112 mM NaCl, 4.7 mM KCl, 2.2 mM CaCl₂, 1.2 mM MgCl₂, 25 mM NaHCO₃, 1.2 mM KH₂PO₄, and 14 mM glucose. The pH was adjusted to 7.4 by gassing with a mixture of 95% O₂-5% CO₂. To suppress the effects of transmitter release from nerve endings in the preparations, all contractility experiments were performed in the presence of the following neurotransmitter antagonists: 1 μM atropine, 1 μM phentolamine, 1 μM propranolol, 1 μM tetrodotoxin, and 10 μM suramin.

Cell isolation. UBSMs of male mice (7- to 13-wk-old) were immersed in Ca²⁺/Mg²⁺-free Krebs solution for 15 min at 37°C. Subsequently, the solution was replaced with Ca²⁺/Mg²⁺-free Krebs solution containing 0.25% collagenase (Amano, Nagoya, Japan) and 0.01% papain (Sigma-Aldrich, St. Louis, MO), and then the tissue was incubated for 30 min at 37°C. After incubation, the solution was replaced with Ca²⁺/Mg²⁺-free Krebs solution. Thereafter, individual myocytes were mechanically dispersed from the tissue fragments by gentle trituration using a glass pipette. All experiments using cells were carried out at room temperature (25°C).

Electrophysiological recording. Electrophysiological studies were performed using a whole cell patch-clamp technique with EPC-7 (List, Darmstadt, Germany) or CEZ-2400 (Nihon Kohden, Tokyo, Japan) amplifiers, an analog-digital converter (Digidata 1440A; Axon, Foster City, CA), and a pCLAMP software (version 10.2; Axon) in single smooth muscle cells, as described previously (19). For recording of NCX current (16), the extracellular solution had an ionic composition of 140 mM *N*-methyl-D-glucamine (NMDG), 1 mM CaCl₂, 1 mM MgCl₂, 0.02 mM ouabain, 0.01 mM nifedipine, and 5 mM HEPES with a pH of 7.4 adjusted with HCl. The pipette solution contained 40 mM NaCl, 10 mM BAPTA, 70 mM CsOH, 30 mM aspartate, 3 mM MgCl₂, 5 mM MgATP, and 10 mM HEPES. The pH was adjusted to 7.2 with NaOH. Myocytes were clamped at a holding potential of -60 mV, and a descending ramp protocol from +15 mV to -100 mV for 500 ms was performed every 10 s. When spontaneous transient outward currents (STOCs) were recorded at a holding potential of -30 mV, normal HEPES-buffered saline solution was used with a composition of 137 mM NaCl, 5.9 mM KCl, 2.2 mM CaCl₂, 1.2 mM MgCl₂, 14 mM glucose, and 10 mM HEPES and a pH of 7.4 adjusted with NaOH. The pipette solution contained 20 mM NaCl,

120 mM KCl, 1 mM MgCl₂, 10 mM HEPES, and 2 mM MgATP and a pH of 7.2 adjusted with KOH.

Ca²⁺ imaging. Cytosolic Ca²⁺ dynamics were imaged using a total internal reflection fluorescence (TIRF) microscope (Eclipse TE2000-U; Nikon) equipped with an objective lens (CFI Plan Apo TIRF ×60/1.45, oil immersion; Nikon), an EM-CCD camera (C9100-12; Hamamatsu Photonics, Hamamatsu, Japan), and AQUACOSMOS software (version 2.6; Hamamatsu Photonics), as reported previously (48, 49). Single UBSM cells were loaded with fluorescent Ca²⁺ indicator, 10 μM fluo-4/AM for 10 min. Ca²⁺ images were acquired every 27.2 ms and a resolution of 107 nm per pixel. The bath contained HEPES-buffered saline solution as indicated above.

Urination patterns. Urination pattern analysis was carried out as reported previously (18). In brief, female mice (13- to 22-wk-old) were placed in standard cages for 3 h with the bedding replaced by a sheet of filter paper. Food and water were freely given. Urine spots were photographed under ultraviolet light. Test mice were given 10 mg/kg KB-R7943 (dissolved in 5% gum arabic solution) by oral administration an hour before the experiments.

Drugs. Pharmacological reagents were obtained from Sigma-Aldrich except for KB-R7943 and SN-6 (Tocris, Ellisville, MO), BAPTA and HEPES (Dojin, Kumamoto, Japan), and CdCl₂, NiCl₂, and ryanodine (Wako, Osaka, Japan). KB-R7943 and SN-6 were dissolved in dimethyl sulfoxide at the concentration of 10 mM as a stock solution.

Statistics. Pooled data are shown as the means ± SE. Statistical significance between the two groups was determined by Student's *t*-test. Significant difference is expressed in the Figs. 1–7 as **P* < 0.05 or ***P* < 0.01.

RESULTS

Enhanced spontaneous contractions in NCX1.3^{tg/tg} UBSM. Spontaneous contractions were measured in UBSM tissue strips from WT and NCX1.3^{tg/tg} mice. Spontaneous contractions were observed in WT tissues in the presence of neurotransmitter antagonists (1 μM atropine, 1 μM phentolamine, 1 μM propranolol, 1 μM tetrodotoxin, and 10 μM suramin), but unexpectedly, they were significantly enhanced in UBSM of NCX1.3^{tg/tg} mice (Fig. 1A). The area under the curve (mN/min; AUC) of contractions for a 5-min recording period was markedly larger in NCX1.3^{tg/tg} (208 ± 43; *n* = 7) compared with WT tissues (22 ± 3; *n* = 3; *P* < 0.01; Fig. 1B). Spontaneous contractions of WT tissues were almost completely blocked by application of 300 nM nicardipine (to 11 ± 2%; *n* = 6; Fig. 1, C and D) but only partially suppressed in NCX1.3^{tg/tg} tissues (to 39 ± 9%; *n* = 8). Spontaneous contractions in NCX1.3^{tg/tg} strips were inhibited by omitting Ca²⁺ from the bath solution or by treatment with 50 μM ryanodine, 100 μM tetracaine, or 10 μM cyclopiazonic acid (*n* = 3–8; *P* < 0.01), but they were not affected by 10 μM xestospongine C, 10 μM La³⁺, or 10 μM Gd³⁺ (*n* = 3–11; Fig. 2). Spontaneous contractions of NCX1.3^{tg/tg} (to 67 ± 9%; *n* = 7; *P* < 0.01), but not WT tissues (to 97 ± 12%; *n* = 3), were significantly reduced by 10 μM KB-R7943 (Fig. 3, A and B) or 1 mM Ni²⁺ (to 11 ± 4%; *n* = 4; *P* < 0.01; Fig. 2B), inhibitors of NCX. Significantly, the nicardipine-resistant, spontaneous contractions of NCX1.3^{tg/tg} were reduced by 10 μM KB-R7943 (to 6 ± 1% of control; *n* = 6; *P* < 0.01 vs. nicardipine; Fig. 3, C and D). Other blockers of NCX activity, 3 μM SN-6 (*n* = 4; Fig. 3, E and F) or 1 mM Ni²⁺ (data not shown), caused a similar attenuation of spontaneous contraction of NCX1.3^{tg/tg} UBSM in the presence of nicardipine.

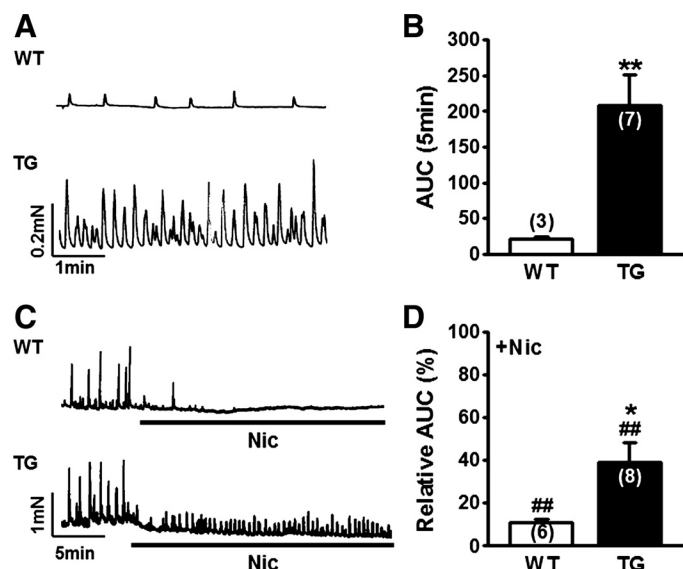


Fig. 1. Enhanced spontaneous contractions in NCX1.3^{tg/tg} urinary bladder smooth muscle (UBSM) tissues. The contribution of Na⁺/Ca²⁺ exchanger (NCX) to spontaneous contractions of UBSM was determined in presence of 1 μ M atropine, 1 μ M phentolamine, 1 μ M propranolol, 1 μ M tetrodotoxin, and 10 μ M suramin to block neuronal modulation. The number of tissue preparations examined is given in parentheses. *A* and *B*: representative recordings of isometric tension development due to spontaneous contractions in wild-type (WT) and NCX1.3^{tg/tg} [transgenic (TG)] UBSM (*A*) and integrated areas of contraction above resting tension level for a 5-min period [area under the curve (AUC); *B*]. *C* and *D*: representative recordings of spontaneous contractions in 300 nM nicardipine (*C*) in WT and NCX1.3^{tg/tg} strips and summarized data of AUC for 5 min (*D*). Note that the nicardipine-insensitive component in NCX1.3^{tg/tg} was significantly larger than WT UBSM. * P < 0.05, ** P < 0.01 vs. WT; ### P < 0.01 vs. before application of nicardipine.

NCX current in NCX1.3^{tg/tg} smooth muscle cells. Whole cell current recordings were made by standard patch-clamp method to detect NCX activity in freshly isolated UBSM cells from WT and NCX1.3^{tg/tg} mice. To facilitate detection of NCX current, the bath and pipette solutions employed were adjusted to favor Na⁺ extrusion and Ca²⁺ influx. Specifically, external Na⁺ and K⁺ were substituted by NMDG in the bathing solution that also contained 1 mM Ca²⁺, 20 μ M ouabain, and 10 μ M nifedipine, and the pipette solution contained Cs⁺ to block outward K⁺ currents, 40 mM Na⁺ and 10 mM BAPTA (16). Figure 4 shows the current-voltage relationship for membrane current in WT and NCX1.3^{tg/tg} myocytes in response to 500-ms descending ramp protocols applied between +15 and -100 mV (0.24 V/s, 10-kHz sampling rate) from a holding potential of -60 mV every 10 s (for clarity all recordings are shown on a standard voltage axis). In WT cells ($n = 4$), an inwardly directed 1 mM Ni²⁺-sensitive current was detected at negative potentials (-9.6 ± 2.1 and 0.6 ± 3.4 pA at -100 and 0 mV, respectively), the reversal potential was -5.9 ± 6.3 mV, and the Ni²⁺-sensitive holding current was inwardly directed at -60 mV (Fig. 4*A*). In contrast, the Ni²⁺-sensitive current of NCX1.3^{tg/tg} cells ($n = 4$) was outwardly directed (-1.8 ± 3.0 and 27.9 ± 3.6 pA at -100 and 0 mV, respectively), the reversal potential was -100.7 ± 10.5 mV ($P < 0.01$), and the holding current was outward at -60 mV (Fig. 4*B*). A similar whole cell NCX current with a reversal potential of -89.9 ± 23.0 mV was detected in NCX1.3^{tg/tg} myocytes using the selective NCX inhibitor KB-R7943 at 10 μ M ($n = 5$; $P < 0.01$; Fig. 4*C*).

Occurrence of long-lasting STOCs in NCX1.3^{tg/tg} cells. At a holding potential of -30 mV, STOCs sensitive to 100 nM iberiotoxin or 1 μ M paxilline ($n = 3$ for each) and due to large-conductance Ca²⁺-activated K⁺ (BK_{Ca}) channel activity were detected in all UBSM cells, but cells of NCX1.3^{tg/tg} mice frequently showed STOCs with different kinetics (Fig. 5*A*). The peak amplitude of STOCs in NCX1.3^{tg/tg} cells (39 ± 5 pA; $n = 11$) was slightly, but not significantly, larger than that in WT cells (28 ± 3 pA $n = 6$; Fig. 5*B*), and there was no significant difference in the frequency of STOCs (Fig. 5*C*). However, the half duration and area of single STOCs in NCX1.3^{tg/tg} cells (73 ± 9 ms and $4,759 \pm 1,008$ pA-ms, respectively; $n = 11$) were significantly larger than those of WT cells (39 ± 3 ms and $1,697 \pm 243$ pA-ms; $n = 6$; $P < 0.05$, respectively; Fig. 5, *D* and *E*). Figure 5*F* shows that STOCs with relatively large area ($>10^4$ pA-ms) were rarely detected in WT cells ($<1\%$ of 140 STOCs from 6 cells),

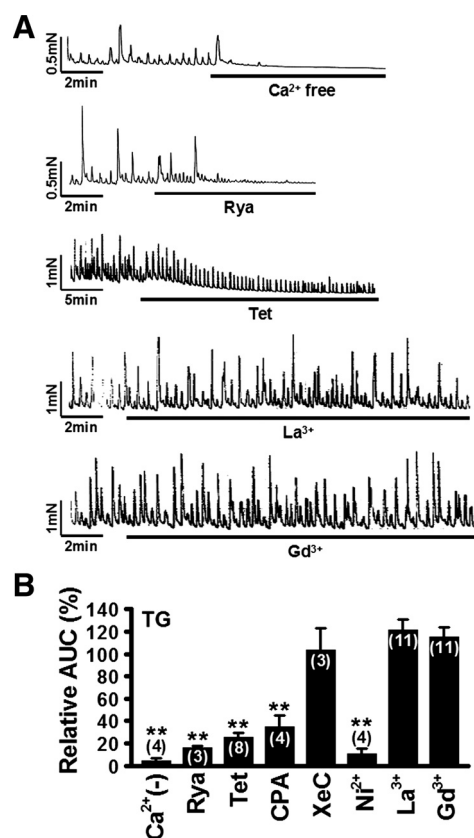


Fig. 2. Ca²⁺ sources of nicardipine-resistant component of spontaneous contractions in NCX1.3^{tg/tg} UBSM tissues. Ca²⁺ sources for the residual spontaneous contractions observed in the presence of 1 μ M nicardipine were examined in UBSM strips from NCX1.3^{tg/tg} (TG). All experiments were performed in the presence of 1 μ M nicardipine. To avoid effects of transmitters released from nerve endings, 1 μ M atropine, 1 μ M phentolamine, 1 μ M propranolol, 1 μ M tetrodotoxin, and 10 μ M suramin were also added to the bathing solution. *A*: representative effects of Ca²⁺-free bath solution, 50 μ M ryanodine, 100 μ M tetracaine, 10 μ M La³⁺, and 10 μ M Gd³⁺ on nicardipine-resistant, spontaneous activity of NCX1.3^{tg/tg} UBSM tissues are shown. *B*: relative AUC above the resting level for a 5-min period was measured after the application of varied solutions and/or blockers (Ca²⁺-free solution, 50 μ M ryanodine, 100 μ M tetracaine, 10 μ M cyclopiazonic acid, 10 μ M xestospongin C, 10 μ M La³⁺, or 10 μ M Gd³⁺) and expressed as a percent of the AUC for nicardipine-resistant component of spontaneous contractions. ** P < 0.01 vs. control.

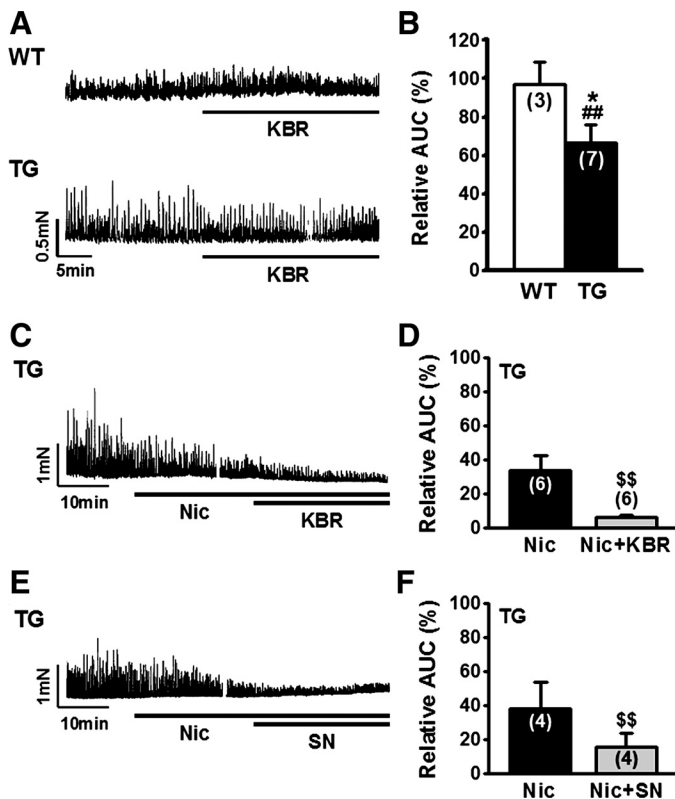


Fig. 3. Effects of KB-R7943 on spontaneous contractions in WT and NCX1.3^{tg/tg} UBSM strips. Effects of KB-R7943 on UBSM tissues in the presence of neurotransmitter inhibitors without and with nifedipine were examined in UBSM strips from WT and NCX1.3^{tg/tg} (TG). *A*: representative effect of 10 μ M KB-R7943 on spontaneous contractions of WT and NCX1.3^{tg/tg} UBSM. *B*: average level of suppression of spontaneous contractility indicated by AUC above the resting level for a 5-min period in the presence of KB-R7943 compared with control period for WT and NCX1.3^{tg/tg} UBSM tissues. Note that KB-R7943 did not affect the spontaneous contractions in WT but significantly suppressed activity in NCX1.3^{tg/tg} strips. *C* and *D*: effects of 10 μ M KB-R7943 on spontaneous contraction in the presence of 1 μ M nifedipine in NCX1.3^{tg/tg} UBSM. *E* and *F*: effects of 3 μ M SN-6 on spontaneous contraction in the presence of nifedipine in NCX1.3^{tg/tg} UBSM. * $P < 0.05$ vs. WT; ## $P < 0.01$ vs. before application of KB-R7943; \$\$ $P < 0.01$ vs. nifedipine alone.

whereas they were frequently observed in NCX1.3^{tg/tg} cells (~10% of 254 STOCs from 11 cells).

Global propagation of local Ca^{2+} transients in NCX1.3^{tg/tg} myocytes. Local Ca^{2+} transients were imaged using a TIRF microscope and UBSM myocytes loaded with the fluorescent Ca^{2+} indicator fluo-4 acetoxymethyl ester (fluo-4/AM, 10 μ M). Spatiotemporally restricted elevations in $[Ca^{2+}]_i$, called Ca^{2+} sparks, occurring independently at several regions within the TIRF visualization area, were detected in all WT and NCX1.3^{tg/tg} myocytes in standard physiological bathing solution (Fig. 6A). The peak amplitude of these Ca^{2+} transients was slightly larger in NCX1.3^{tg/tg} cells (F/F_0 : $1.7 \pm 0.1\%$; $n = 62$) compared with WT cells ($1.2 \pm 0.1\%$; $n = 26$; $P < 0.05$; Fig. 6B), but there was no difference in their frequency or the number of sites/TIRF area (Fig. 6, C and D). Significantly, however, 1) the average maximum area of the Ca^{2+} transients in NCX1.3^{tg/tg} cells ($18.9 \pm 1.6 \mu m^2$; $n = 469$) was significantly larger than that in WT cells ($4.3 \pm 0.5 \mu m^2$; $n = 168$; $P < 0.01$; Fig. 6E); and 2) global elevations in $[Ca^{2+}]_i$ within

the TIRF visualization area were rarely observed in WT cells, but Ca^{2+} spark-triggered propagating elevations in $[Ca^{2+}]_i$ leading to a global increase were frequently observed in NCX1.3^{tg/tg} cells. Based on the distribution histogram of maximum area shown in Fig. 6F, it is clear that Ca^{2+} transients with relatively large propagation covering $>20 \mu m^2$ and reminiscent of propagating Ca^{2+} waves were rare in WT cells ($<1\%$ of 168 events from 5 cells) but were ~20% of the events in NCX1.3^{tg/tg} cells (469 events from 9 cells). To address the role of enhanced NCX activity as a cause of the abnormal Ca^{2+} events in NCX1.3^{tg/tg} myocytes, the effects of KB-R7943 were examined under identical recording conditions. Following treatment with 10 μ M KB-R7943, the large propagating Ca^{2+} transients disappeared, but Ca^{2+} sparks still remained ($n = 7$). Exposure to 10 μ M ryanodine plus 100 μ M Cd^{2+} abolished all changes in $[Ca^{2+}]_i$ in NCX1.3^{tg/tg} cells ($n = 4$).

Overactive bladder in NCX1.3^{tg/tg} mice. The possibility that NCX overexpression affected the pattern of urination was examined using WT and NCX1.3^{tg/tg} mice. When the urination

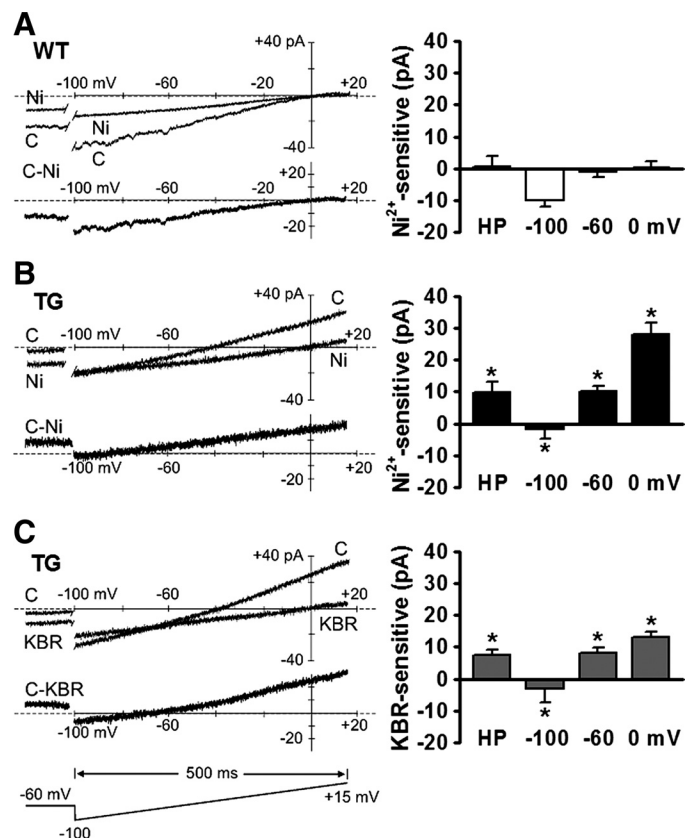


Fig. 4. NCX currents in smooth muscle cells from NCX1.3^{tg/tg} urinary bladder. NCX currents were recorded from freshly isolated myocytes from WT and NCX1.3^{tg/tg} UBSM (TG). Myocytes were voltage-clamped at a holding potential (HP) of -60 mV, and a 500-ms descending ramp protocol from $+15$ mV to -100 mV was applied every 10 s. *A*: representative recordings of whole cell current before (C) and after (Ni) application of 1 mM Ni^{2+} and Ni^{2+} -sensitive difference current (C-Ni) for WT myocyte. The reversal potential of Ni^{2+} -sensitive component was ~ 0 mV and average difference current amplitudes at -100 , -60 , and 0 mV are shown at right. *B* and *C*: representative recordings of whole cell currents and difference currents for NCX1.3^{tg/tg} myocytes presence of 1 mM Ni^{2+} (*B*) or 10 μ M KB-R7943 (*C*). The reversal potential of Ni^{2+} - and KB-R7943-sensitive components was ~ -95 mV. Average difference current amplitudes at -100 , -60 , and 0 mV are shown at right in *B* and *C*. Data were obtained from 4 to 5 cells in each group. * $P < 0.05$ vs. WT.

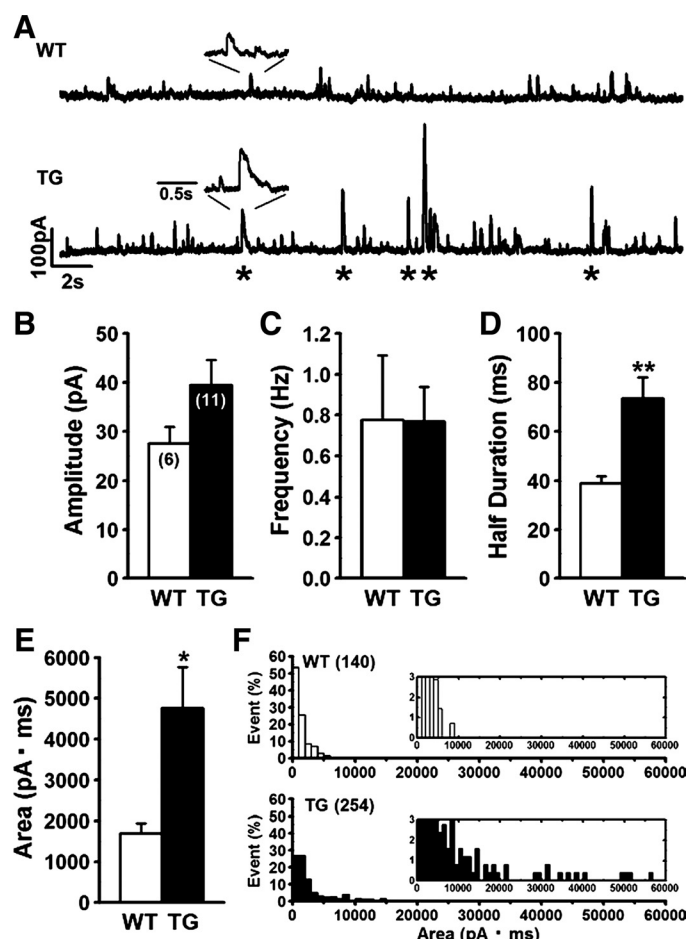


Fig. 5. Spontaneous transient outward currents (STOCs) in NCX1.3^{tg/tg} myocytes. STOCs were measured at a holding potential of -30 mV under whole cell voltage clamp in UBSM cells from WT and NCX1.3^{tg/tg} (TG) mice. *A*: representative recordings of STOCs in WT and NCX1.3^{tg/tg} myocytes with expanded traces showing abnormal kinetics of STOCs in transgenic compared with WT mouse myocyte. *B–E*: data of peak amplitude (*B*), frequency (*C*), half duration (*D*), and area (*E*) of STOCs at -30 mV in WT and NCX1.3^{tg/tg} cells. *F*: distribution histogram of STOC events expressed as area. *Inset*: enlarged histogram for y-axis. Note that STOCs with relatively large area ($>10^4$ pA·ms, indicated by * in *A*) were rare in WT cells but $\sim 10\%$ of events in NCX1.3^{tg/tg} cells. * $P < 0.05$, ** $P < 0.01$ vs. WT.

pattern of freely moving mice was recorded for 3 h, the number of spots of urine created by NCX1.3^{tg/tg} mice (5.3 ± 1.4 ; $n = 14$) was larger than that of WT mice (1.4 ± 0.4 ; $n = 8$; $P < 0.05$; Fig. 7, *A* and *B*). There was no significant difference in the number of large urine spots (>1 cm²) or in the total area of spots between the groups of mice, but the number of small spots (<1 cm²) produced by NCX1.3^{tg/tg} mice was larger (4.1 ± 1.3 ; $n = 14$), and the average area of individual spots (3.5 ± 0.8 cm²; $n = 74$) was significantly smaller than those of WT mice (0.4 ± 0.2 ; $n = 8$; $P < 0.05$; and 12.2 ± 3.5 cm²; $n = 11$; $P < 0.01$ respectively; Fig. 7*C*). The effect of KB-R7943 on urination was examined to determine whether the different pattern observed for NCX1.3^{tg/tg} mice was related to NCX activity. When the analysis was initiated after 1 h of oral administration of 10 mg/kg KB-R7943, the numbers of large and small urine spots, as well as the average area of individual spots produced by NCX1.3^{tg/tg} mice, was identical to that of WT mice.

Urination pattern in G833C-NCX1.3^{tg/tg} mice. Finally, the pattern of urination in the absence and presence of KB-R7943 was examined using G833C-NCX1.3^{tg/tg} mice that have a KB-R7943-insensitive mutation of NCX1.3. In G833C-NCX1.3^{tg/tg} mice, the number of spots of urine (7.7 ± 0.7 ; $n = 12$), the number of large urine spots (2.7 ± 0.1 ; $n = 12$), and the number of small spots (5.0 ± 0.7 ; $n = 12$) were similar to those produced by NCX1.3^{tg/tg} mice ($P > 0.05$; Fig. 8*A*). There was no significant difference in the total area of spots (33.9 ± 1.6 cm²; $n = 12$) and the average area of individual spots (4.9 ± 0.5 cm²; $n = 92$) between the groups of mice ($P > 0.05$; Fig. 8*B*). Furthermore, all urinary parameters for G833C-NCX1.3^{tg/tg} mice were not affected by oral administration of 10 mg/kg KB-R7943 ($n = 8$; $P > 0.05$). These data indicate that the pattern of more frequent, smaller volumes of urine produced by NCX1.3^{tg/tg} mice was reversed by the inhibition of NCX activity.

DISCUSSION

The study addresses the effect of overexpression of NCX1.3 on membrane excitability and cytosolic Ca²⁺ mobilization in isolated UBSM myocytes, spontaneous contractions of UBSM tissues, and regulation of urinary bladder function. Here, we report that smooth muscle-specific NCX overexpression was associated with 1) enhanced spontaneous UBSM contractions; 2) an outwardly directed KB-R7943- and Ni²⁺-sensitive NCX current with a reversal potential (NCX_{rev}) of between -90 and -100 mV; 3) STOCs and Ca²⁺ sparks of prolonged duration, with the latter frequently exhibiting propagation in the form of Ca²⁺ wave-like events; and 4) alterations in the pattern of urination in freely moving mice consistent with overactive bladder (OAB) syndrome. These findings have important implications concerning the role of Ca²⁺ influx via reverse mode NCX in control of UBSM contractility.

It is widely accepted that NCX plays an important role as a mechanism for Ca²⁺ extrusion following global increases [Ca²⁺]_i in smooth muscle myocytes, despite the fact that NCX expression in these cells is much lower than that in cardiac muscle (9, 27, 51). For example, the duration of Ca²⁺ transients evoked by serotonin stimulation is increased after pretreatment of cultured vascular myocytes with antisense oligonucleotides against NCX1 (42), and Na⁺-dependent vascular dilation is reduced in heterozygous NCX1 knockout (NCX1^{+/-}) mice (45). Based on these results, it was suggested that NCX principally operates in the forward mode to extrude Ca²⁺ in smooth muscle cells under normal physiological conditions. Accordingly, our previous study demonstrated that NCX1.3^{tg/tg} UBSM expressed a fourfold greater level of NCX1 protein compared with WT UBSM and that NCX1.3 overexpression potentiated the ability of forward mode Ca²⁺ efflux to reduce the amplitude of the plateau phase of contractions induced by acetylcholine, high K⁺, or direct electrical stimulation (32).

However, reverse mode activity of the NCX was also proposed to be important for smooth muscle function (3, 12, 17, 39, 40). Inhibition of NCX with KB-R7943 decreased [Ca²⁺]_i responses evoked by agonists or store depletion in smooth muscles (11, 17, 56), and SEA0400 decreased [Ca²⁺]_i and evoked vasodilation of arteries precontracted with ouabain or following a reduction in [Na⁺]_o (23, 39). More recently, Ca²⁺

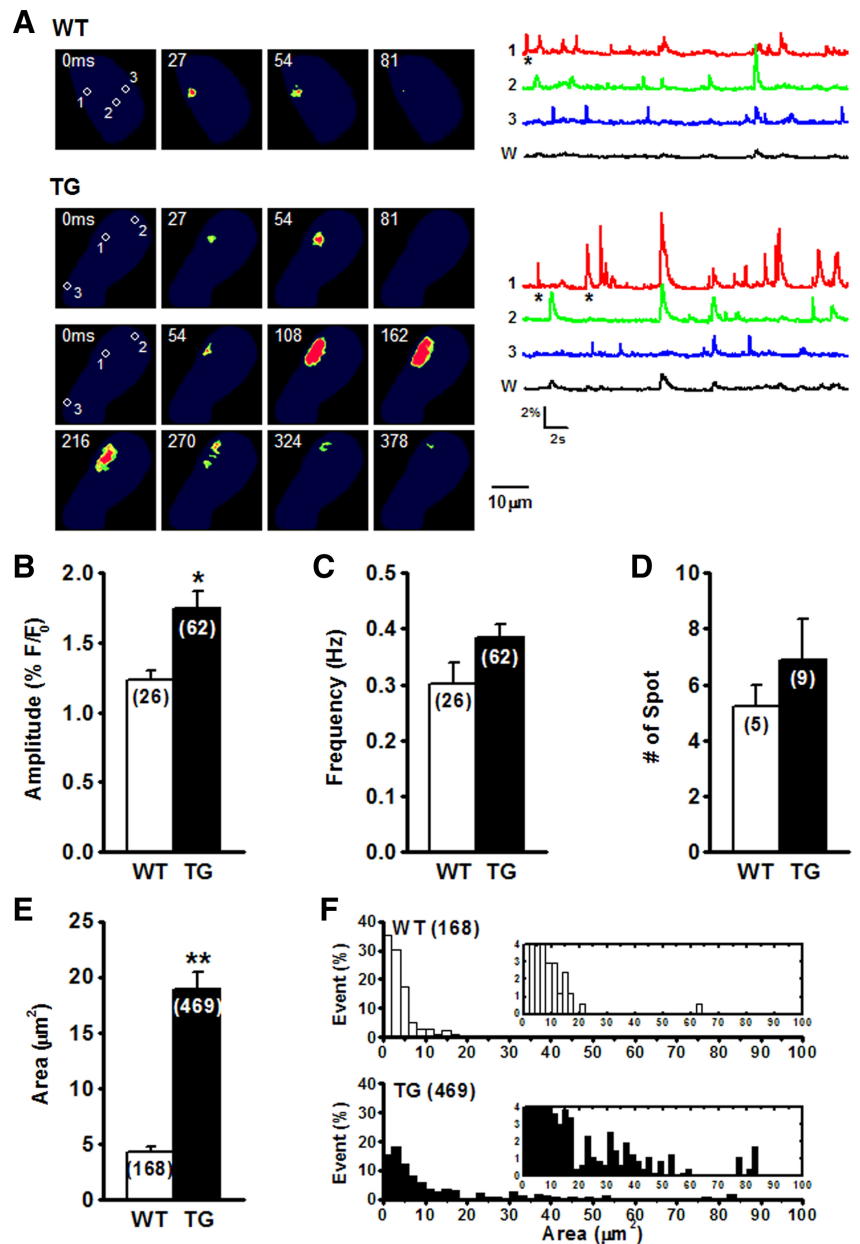


Fig. 6. Abnormal Ca^{2+} mobilization in $\text{NCX1.3}^{\text{tg/tg}}$ myocytes. Local Ca^{2+} transients of WT and $\text{NCX1.3}^{\text{tg/tg}}$ (TG) UBSM cells were imaged using a total internal reflection fluorescence (TIRF) microscope and $10 \mu\text{M}$ fluo-4/AM. **A**: representative Ca^{2+} images in WT and $\text{NCX1.3}^{\text{tg/tg}}$ cells within TIRF zone are sequentially shown (*left*). Traces of local $[\text{Ca}^{2+}]$ changes correspondingly indicated as “1, 2, 3” in images are plotted against time (*right*). Ca^{2+} changes in global area are plotted as “W.” Note that Ca^{2+} sparks occurred in both types of cells (indicated by 1st * in WT and TG), but Ca^{2+} propagation triggered by Ca^{2+} spark (2nd * in TG) was occasionally observed in $\text{NCX1.3}^{\text{tg/tg}}$ cells. **B–E**: data of peak amplitude (**B**), frequency (**C**), number of spark sites (**D**), and area (maximum area of Ca^{2+} propagation; **E**) of Ca^{2+} transients in WT and $\text{NCX1.3}^{\text{tg/tg}}$ cells. **F**: distribution histogram of Ca^{2+} events is plotted against area. *Inset*: enlarged histogram for y-axis. Note that Ca^{2+} transients with large area propagating as Ca^{2+} waves ($>20 \mu\text{m}^2$) were rare in WT cells but $\sim 20\%$ of events in $\text{NCX1.3}^{\text{tg/tg}}$ cells. * $P < 0.05$, ** $P < 0.01$ vs. WT.

entry via NCX1 and $[\text{Ca}^{2+}]_i$ were shown to be reduced and associated with a reduction in arterial myogenic tone and blood pressure in smooth muscle-specific NCX1-null mice ($\text{NCX1}^{\text{SM-/-}}$; Ref. 54). These findings suggest that the reverse mode of NCX is also important in the regulation of smooth muscle function under physiological conditions.

The present study was initiated by the finding that NCX overexpression enhanced spontaneous contractions of UBSM. In UBSM cells, membrane excitability and Ca^{2+} influx through VDCC and CICR play a crucial role in the regulation of myogenic contraction (26). Consistent with this view, we found that spontaneous contractions of UBSM from WT mice were almost completely suppressed by nifedipine or ryanodine, as was reported previously (18, 31). However, nifedipine only partially suppressed spontaneous activity of $\text{NCX1.3}^{\text{tg/tg}}$ tissues, and the residual, nifedipine-resistant contractions of $\text{NCX1.3}^{\text{tg/tg}}$ tissues were not affected by La^{3+} or Gd^{3+} , but they were

dependent on extracellular Ca^{2+} ($[\text{Ca}^{2+}]_o$), suggesting the participation of an additional Ca^{2+} entry pathway not involving VDCC or nonselective cation channels. The nifedipine-insensitive spontaneous contractions in $\text{NCX1.3}^{\text{tg/tg}}$ UBSM were susceptible to inhibition by KB-R7943, SN-6, and Ni^{2+} implied the possibility that this Ca^{2+} entry pathway was dependent on the NCX operating in the reverse mode (24, 47).

The presence of a detectable KB-R7943- and Ni^{2+} -sensitive outward current in conditions favoring reverse mode NCX activity in myocytes isolated from $\text{NCX1.3}^{\text{tg/tg}}$, but not WT mice, is consistent with the view that Ca^{2+} influx due to reverse mode NCX is greater in UBSM of the genetically modified mice. To our knowledge, the data presented in Fig. 4 represent the first quantitative recordings of NCX current in smooth muscle. Detection of NCX currents in smooth muscle cells has presented difficulties in the past, presumably owing to the relatively low level of NCX protein expression compared

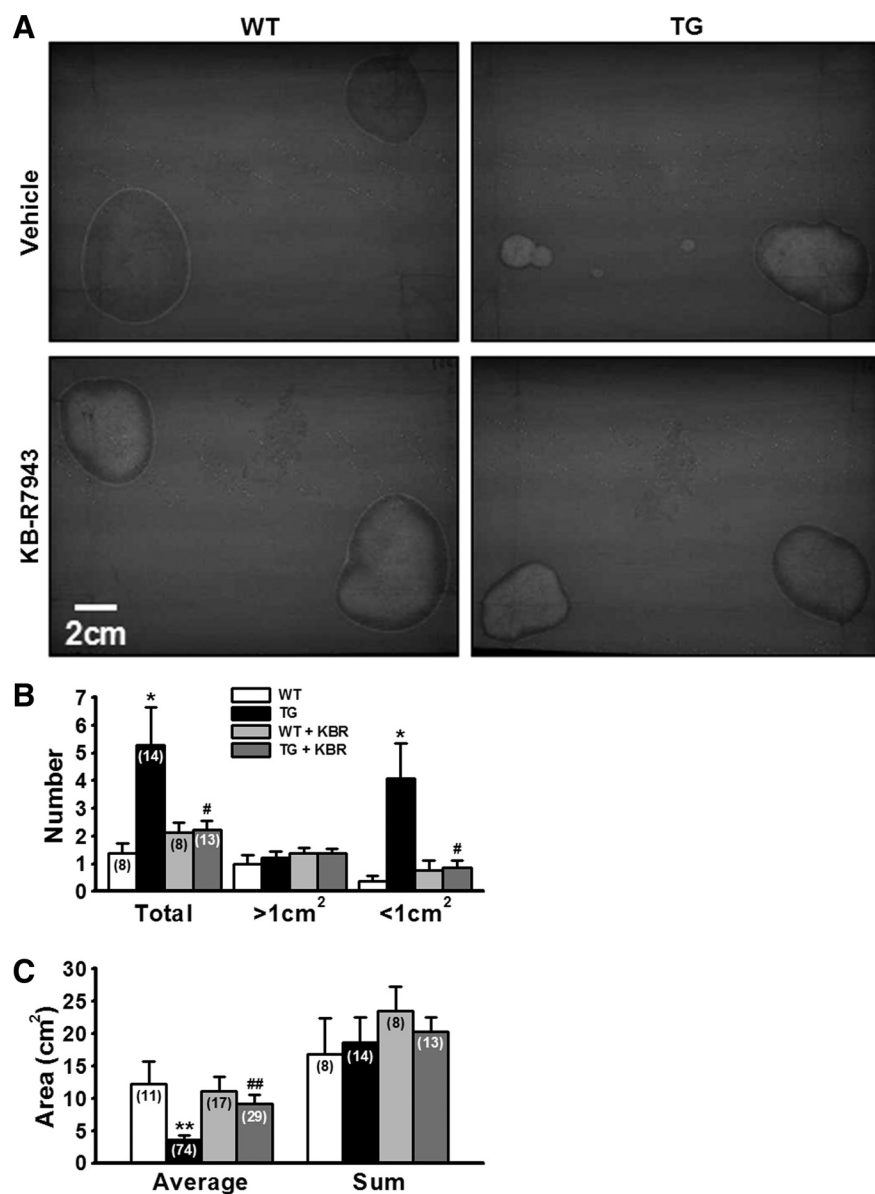


Fig. 7. Urination pattern of WT vs. NCX1.3^{tg/tg} mice. The possibility that NCX overexpression affected urination was examined over a 3-h period using freely-moving female WT and NCX1.3^{tg/tg} (TG) mice by collection of urine on filter paper. A: representative urination pattern of WT and NCX1.3^{tg/tg} mice under the control conditions (vehicle) and 1 h after oral administration of 10 mg/kg KB-R7943. B: total spot number (total) and number of large (>1 cm²) and small (<1 cm²) spots. C: average area of individual urination spots and average total area of urine spots. Note that more frequent urination of smaller spots exhibited by NCX1.3^{tg/tg} mice was reversed by oral administration of KB-R7943. **P* < 0.05, ***P* < 0.01 vs. WT; #*P* < 0.05, ##*P* < 0.01 vs. vehicle.

with other excitable cells, such as cardiac myocytes. Here, we detected a KB-R7943- and Ni²⁺-sensitive outward current that reversed approximately -95 mV in NCX1.3^{tg/tg} cells, but a similar conductance was not apparent in WT cells. Rather, the Ni²⁺-sensitive difference current of WT myocytes was inwardly directed at negative voltages, reversed at ~0 mV, and was likely due to gating of Ca²⁺ permeable nonselective cation channels. The reversal potential of the KB-R7943- and Ni²⁺-sensitive current of NCX1.3^{tg/tg} cells does not correspond to that expected for a nonselective cation conductance, but it was also positive to the predicted value for NCX_{rev} based on the bath and pipette solutions employed and a Na⁺-Ca²⁺ transport ratio of 3:1 (i.e., negative to -150 mV assuming a contaminating level of [Na⁺]_o, [Na⁺]_i of 40 mM, [Ca²⁺]_o of 1 mM, [Ca²⁺]_i of 1–10 nM with 10 mM BAPTA and no added Ca²⁺; Ref. 16). We attribute this discrepancy to the labile nature of NCX_{rev} and that it can deviate considerably from predicted values when cells are maintained in nonequilibrium conditions (5). In the present experiments, UBSM myocytes were held at

-60 mV (500-ms ramp protocols were applied every 10 s); this is considerably positive to the predicted value of NCX_{rev}, and an outwardly directed KB-R7943- and Ni²⁺-sensitive holding current was detected indicative of steady-state Na⁺ efflux and Ca²⁺ influx, i.e., steady-state reverse mode NCX activity. Given the dissipative nature of NCX activity, this steady-state current would be expected to alter [Na⁺]_o and [Ca²⁺]_i and, thereby, NCX_{rev} due to local accumulation within diffusion-restricted microdomains, such as within caveolae (extracellularly) and sites of close apposition between the junctional sarcoplasmic reticulum (SR) and the plasma membrane (intracellularly; Refs 5, 7).

The present findings are consistent with the view that overexpression of NCX in smooth muscle cells leads to abnormal [Ca²⁺]_i dynamics and increased spontaneous contractions as a result of enhanced reverse mode NCX activity. Specifically, that enhanced reverse mode activity increases spontaneous Ca²⁺ release from SR stores leading to propagating Ca²⁺ wave-like events that initiate spontaneous contractions. We do

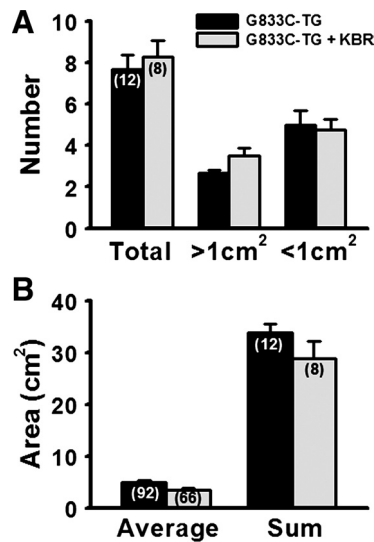


Fig. 8. Urination pattern of G833C-NCX1.3^{tg/tg} mice. The pattern analysis of urination in the absence and presence of KB-R7943 was examined over a 3-h period using freely moving female G833C-NCX1.3^{tg/tg} (G833C-TG) mice that have a KB-R7943-insensitive mutation of NCX1.3. The urine from G833C-NCX1.3^{tg/tg} mice under the control conditions (vehicle) and 1 h after oral administration of 10 mg/kg KB-R7943 was collected on filter paper. *A*: total spot number (total) and number of large (>1 cm²) and small (<1 cm²) spots. *B*: average area of individual urination spots and average total area of urine spots. Note that the more frequent urination of smaller spots exhibited by G833C-NCX1.3^{tg/tg} mice was not improved by oral administration of KB-R7943.

not attribute the enhanced spontaneous contractility of NCX1.3^{tg/tg} tissues to an increase in membrane excitability. This view is based on the following line of reasoning: BK_{Ca} channels in UBSMs are known to be activated by 1) membrane depolarization and the rise in [Ca²⁺]_i associated with action potential firing (13, 21, 31, 49); and 2) local subplasmalemmal elevations in [Ca²⁺]_i, referred to as Ca²⁺ sparks, owing to release from ryanodine receptors (RyRs) in the SR (15, 31, 35, 53). STOCs arising from BK_{Ca} channel activity evoked by Ca²⁺ sparks are thought to maintain resting membrane potential at a hyperpolarized level to suppress VDCC activity, lower [Ca²⁺]_i, and inhibit contractility; i.e., Ca²⁺ spark/BK_{Ca} channel coupling plays a crucial role in the negative feedback regulation of membrane excitability, resting [Ca²⁺]_i, and contraction of UBSM (20, 25). Accordingly, elevated UBSM contractility and OAB syndrome are observed following BK_{Ca} channel inhibition with iberiotoxin and in genetic BK_{Ca} channel null mice (14, 29). Here, we found that Ca²⁺ transients of longer duration and increased propagation were associated with STOCs of increased duration in NCX1.3^{tg/tg} UBSM myocytes. This change in STOC duration would be expected to reduce membrane excitability, but we observed enhanced spontaneous contractility in NCX1.3^{tg/tg} UBSM tissues. STOCs are occasionally influenced by global Ca²⁺ release (e.g., Ca²⁺ release from SR stores by caffeine or agonists), which often results in smooth muscle contraction (8, 34, 50). Furthermore, VDCC block with nifedipine completely suppressed spontaneous contractions in WT but not NCX1.3^{tg/tg} UBSM tissues, implying that a change in membrane excitability was not involved. Also, we found no differences in the expression of mRNA and protein for VDCC (α_{1C}-subunit), BK_{Ca} channel (α-subunit), transient receptor potential canonical channel (TRPC3), RyRs

(RyR2 and RyR3), and inositol 1,4,5-trisphosphate receptor (IP₃R1) in WT and NCX1.3^{tg/tg} UBSM (data not shown), and the current-voltage relationships of VDCC (100 μM Cd²⁺ sensitive at 0 mV: WT, 5.6 ± 1.1 pA/pF, n = 5; NCX1.3^{tg/tg}, 5.4 ± 1.3 pA/pF, n = 5) and BK_{Ca} (1 μM paxilline-sensitive pCa 6.5 at +60 mV: WT, 34 ± 12 pA/pF, n = 4; NCX1.3^{tg/tg}, 38 ± 11 pA/pF, n = 5) currents were similar (P > 0.05).

On the other hand, we did detect the presence of abnormal [Ca²⁺]_i dynamics involving enhanced SR Ca²⁺ release leading to propagating Ca²⁺ wave-like events and global elevations in [Ca²⁺]_i within the TIRF visualization area in NCX1.3^{tg/tg} myocytes that can be attributed to enhanced NCX reverse mode activity. The frequency of Ca²⁺ sparks and number of spark sites per cell were similar in myocytes of NCX1.3^{tg/tg} and WT mice, but the amplitude and duration of the transients were larger, and propagation of Ca²⁺ sparks leading to a global rise in [Ca²⁺]_i over the TIRF visualization area occurred more frequently in NCX1.3^{tg/tg} cells. These differences in [Ca²⁺]_i dynamics were abolished by inhibition of NCX with KB-R7943 or SR Ca²⁺ release with ryanodine or tetracaine, as were the nifedipine-resistant spontaneous contractions of NCX1.3^{tg/tg} UBSM tissues. The enhanced Ca²⁺ release detected in NCX1.3^{tg/tg} UBSM myocytes is presumably mediated by overfilling of the SR owing to enhanced Ca²⁺ influx through NCX reverse mode, as CICR triggered by NCX reverse mode activity was previously reported in Na⁺-loaded coronary arterial smooth muscle cells (12). Transgenic mice with doxycycline withdrawal-induced cardiac NCX1 overexpression exhibit increased SR Ca²⁺ content and larger Ca²⁺ transients (46), but SR Ca²⁺ content measured by caffeine-induced Ca²⁺ transients was not changed in NCX1.3^{tg/tg} UBSM myocytes (32). However, the possibility that Ca²⁺ content in superficial, subplasmalemmal SR, which is preferentially filled by Ca²⁺ influx via reverse mode NCX (7, 44), is larger in NCX1.3^{tg/tg} cells is indicated by the increased amplitude and duration of the Ca²⁺ transients/sparks.

The most impressive finding of the present study was that NCX1.3^{tg/tg} mice exhibited frequent urination and the phenotype was greatly improved by the oral administration of KB-R7943. Urination pattern analysis showed that smaller volumes of urine were excreted more frequently in NCX1.3^{tg/tg} mice than WT mice, while the total urine volume was comparable. OAB is a syndrome characterized by urinary urgency and is usually associated with increased daytime frequency and/or nocturia (2) that affects ~17% of adults in the United States and Europe (30, 43). OAB symptoms are often associated with UBSM overactivity, and there is currently a lack of effective therapeutic agents to correct this disorder. Muscarinic receptor antagonists that impair UBSM contractility are the main option, but they have limited effectiveness and undesirable side effects (1, 23). In recent years, β₃-adrenoceptor agonists, purinergic receptor antagonists, phosphodiesterase inhibitors, and K⁺ channel openers have all been considered to be potential candidates for the treatment of OAB syndrome (10). In this study, urinary pattern analysis using G833C-NCX1.3^{tg/tg} mice, in which the G833C mutation confers a resistance to KB-R7943-mediated inhibition (22), failed to reproduce the inhibitory effect of KB-R7943 on frequent urination detected in NCX1.3^{tg/tg} mice. These data are consistent with the view that the effect of KB-R7943 on urination in the NCX1.3^{tg/tg} mice may be attributed to suppression of NCX activity, rather than a nonselective effect on another mechanism relevant to the regulation of Ca²⁺

homeostasis. Our findings suggest, therefore, that selective, potent inhibitors of NCX1 could also be considered as a potential therapy for OAB syndrome due to enhanced UBSM contractility, whereas the relevance between NCX overexpression and human OAB remains to be determined.

In conclusion, NCX in UBSM can work in both forward and reverse modes under physiological conditions. Overexpression of NCX impairs the central role of Ca^{2+} sparks to reduce membrane excitability and global $[\text{Ca}^{2+}]_i$ via generation of STOCs, because overfilling of superficial stores due to enhanced Ca^{2+} influx via reverse mode NCX results in Ca^{2+} sparks of increased amplitude and duration that propagate, triggering further Ca^{2+} release by CICR to elevate global $[\text{Ca}^{2+}]_i$ and evoke spontaneous contractions in NCX1.3^{tg/tg} cells. The enhanced spontaneous contractions of UBSM provoke the OAB symptom of frequent, small volume urination that is effectively suppressed by NCX inhibition with KB-7943.

GRANTS

This work was supported by a Grant-in-Aid for Scientific Research on Priority Areas (20056027; to Y. Imaizumi) from the Ministry of Education, Culture, Sports, Science and Technology; Grants-in-Aid for Scientific Research (B) (20390027 and 23390020; to Y. Imaizumi) and (C) (22590254; to S. Kita, 23590319; to T. Iwamoto) and Grants-in-Aid for Young Scientists (B) (21790087 and 23790092; to H. Yamamura) from the Japan Society for the Promotion of Science. This work was also supported by a Grant-in-Aid from Takeda Science Foundation and a Grant-in-Aid for Research in Nagoya City University (to H. Yamamura). W. C. Cole and Y. Imaizumi were supported by a Grant for International Research Collaboration from Nagoya City University. W. C. Cole is supported by a grant from the Canadian Institutes of Health Research (MOP-97988).

DISCLOSURES

No conflicts of interest, financial or otherwise, are declared by the author(s).

AUTHOR CONTRIBUTIONS

Author contributions: H.Y., W.C.C., S.K., H.M., S.O., T.I., and Y.I. conception and design of research; H.Y., W.C.C., S.K., S.H., H.M., and Y.S. performed experiments; H.Y., W.C.C., S.K., S.H., H.M., Y.S., S.O., and Y.I. analyzed data; H.Y., W.C.C., S.K., S.H., H.M., Y.S., S.O., T.I., and Y.I. interpreted results of experiments; H.Y., W.C.C., S.K., S.H., H.M., Y.S., and T.I. prepared figures; H.Y. and Y.I. drafted manuscript; H.Y., W.C.C., S.O., T.I., and Y.I. edited and revised manuscript; H.Y., W.C.C., S.K., S.H., H.M., Y.S., S.O., T.I., and Y.I. approved final version of manuscript.

REFERENCES

- Abrams P, Andersson KE. Muscarinic receptor antagonists for overactive bladder. *BJU Int* 100: 987–1006, 2007.
- Abrams P, Cardozo L, Fall M, Griffiths D, Rosier P, Ulmsten U, Van Kerrebroeck P, Victor A, Wein A. The standardisation of terminology in lower urinary tract function: report from the standardisation sub-committee of the International Continence Society. *Urology* 61: 37–49, 2003.
- Ashida T, Blaustein MP. Regulation of cell calcium and contractility in mammalian arterial smooth muscle: the role of sodium-calcium exchange. *J Physiol* 392: 617–635, 1987.
- Bers DM. Cardiac excitation-contraction coupling. *Nature* 415: 198–205, 2002.
- Bers DM, Ginsburg KS. Na:Ca stoichiometry and cytosolic Ca-dependent activation of NCX in intact cardiomyocytes. *Ann NY Acad Sci* 1099: 326–338, 2007.
- Blaustein MP, Lederer WJ. Sodium/calcium exchange: its physiological implications. *Physiol Rev* 79: 763–854, 1999.
- Blaustein MP, Wier WG. Local sodium, global reach: filling the gap between salt and hypertension. *Circ Res* 101: 959–961, 2007.
- Bolton TB, Imaizumi Y. Spontaneous transient outward currents in smooth muscle cells. *Cell Calcium* 20: 141–152, 1996.
- Bradley KN, Flynn ER, Muir TC, McCarron JG. Ca^{2+} regulation in guinea-pig colonic smooth muscle: the role of the Na^+ - Ca^{2+} exchanger and the sarcoplasmic reticulum. *J Physiol* 538: 465–482, 2002.
- Chess-Williams R. Potential therapeutic targets for the treatment of detrusor overactivity. *Expert Opin Ther Targets* 8: 95–106, 2004.
- Fellner SK, Arendshorst WJ. Angiotensin II-stimulated Ca^{2+} entry mechanisms in afferent arterioles: role of transient receptor potential canonical channels and reverse Na^+ / Ca^{2+} exchange. *Am J Physiol Renal Physiol* 294: F212–F219, 2008.
- Ganitkevich V, Isenberg G. Ca^{2+} entry through Na^+ - Ca^{2+} exchange can trigger Ca^{2+} release from Ca^{2+} stores in Na^+ -loaded guinea-pig coronary myocytes. *J Physiol* 468: 225–243, 1993.
- Heppner TJ, Bonev AD, Nelson MT. Ca^{2+} -activated K^+ channels regulate action potential repolarization in urinary bladder smooth muscle. *Am J Physiol Cell Physiol* 273: C110–C117, 1997.
- Herrera GM, Heppner TJ, Nelson MT. Regulation of urinary bladder smooth muscle contractions by ryanodine receptors and BK and SK channels. *Am J Physiol Regul Integr Comp Physiol* 279: R60–R68, 2000.
- Herrera GM, Heppner TJ, Nelson MT. Voltage dependence of the coupling of Ca^{2+} sparks to BK_{Ca} channels in urinary bladder smooth muscle. *Am J Physiol Cell Physiol* 280: C481–C490, 2001.
- Hinata M, Yamamura H, Li L, Watanabe Y, Watano T, Imaizumi Y, Kimura J. Stoichiometry of Na^+ - Ca^{2+} exchange is 3:1 in guinea-pig ventricular myocytes. *J Physiol* 545: 453–461, 2002.
- Hirota S, Pertens E, Janssen LJ. The reverse mode of the Na^+ / Ca^{2+} exchanger provides a source of Ca^{2+} for store refilling following agonist-induced Ca^{2+} mobilization. *Am J Physiol Lung Cell Mol Physiol* 292: L438–L447, 2007.
- Hotta S, Morimura K, Ohya S, Muraki K, Takeshima H, Imaizumi Y. Ryanodine receptor type 2 deficiency changes excitation-contraction coupling and membrane potential in urinary bladder smooth muscle. *J Physiol* 582: 489–506, 2007.
- Imaizumi Y, Muraki K, Watanabe M. Ionic currents in single smooth muscle cells from the ureter of the guinea-pig. *J Physiol* 411: 131–159, 1989.
- Imaizumi Y, Ohi Y, Yamamura H, Ohya S, Muraki K, Watanabe M. Ca^{2+} spark as a regulator of ion channel activity. *Jpn J Pharmacol* 80: 1–8, 1999.
- Imaizumi Y, Torii Y, Ohi Y, Nagano N, Atsuki K, Yamamura H, Muraki K, Watanabe M, Bolton TB. Ca^{2+} images and K^+ current during depolarization in smooth muscle cells of the guinea-pig vas deferens and urinary bladder. *J Physiol* 510: 705–719, 1998.
- Iwamoto T, Inoue Y, Ito K, Sakaue T, Kita S, Katsuragi T. The exchanger inhibitory peptide region-dependent inhibition of Na^+ / Ca^{2+} exchange by SN-6 [2-[4-(4-nitrobenzyloxy)benzyl]thiazolidine-4-carboxylic acid ethyl ester], a novel benzyloxyphenyl derivative. *Mol Pharmacol* 66: 45–55, 2004.
- Iwamoto T, Kita S, Zhang J, Blaustein MP, Arai Y, Yoshida S, Wakimoto K, Komuro I, Katsuragi T. Salt-sensitive hypertension is triggered by Ca^{2+} entry via Na^+ / Ca^{2+} exchanger type-1 in vascular smooth muscle. *Nat Med* 10: 1193–1199, 2004.
- Iwamoto T, Watano T, Shigekawa M. A novel isothiourea derivative selectively inhibits the reverse mode of Na^+ / Ca^{2+} exchange in cells expressing NCX1. *J Biol Chem* 271: 22391–22397, 1996.
- Jaggard JH, Porter VA, Lederer WJ, Nelson MT. Calcium sparks in smooth muscle. *Am J Physiol Cell Physiol* 278: C235–C256, 2000.
- Karaki H, Ozaki H, Hori M, Mitsui-Saito M, Amano K, Harada K, Miyamoto S, Nakazawa H, Won KJ, Sato K. Calcium movements, distribution, and functions in smooth muscle. *Pharmacol Rev* 49: 157–230, 1997.
- Karashima E, Nishimura J, Iwamoto T, Hirano K, Hirano M, Kita S, Harada M, Kanaide H. Involvement of Na^+ - Ca^{2+} exchanger in cAMP-mediated relaxation in mice aorta: evaluation using transgenic mice. *Br J Pharmacol* 150: 434–444, 2007.
- Ladilov Y, Haffner S, Balsler-Schäfer C, Maxeiner H, Piper HM. Cardioprotective effects of KB-7943: a novel inhibitor of the reverse mode of Na^+ / Ca^{2+} exchanger. *Am J Physiol Heart Circ Physiol* 276: H1868–H1876, 1999.
- Meredith AL, Thorneloe KS, Werner ME, Nelson MT, Aldrich RW. Overactive bladder and incontinence in the absence of the BK large conductance Ca^{2+} -activated K^+ channel. *J Biol Chem* 279: 36746–36752, 2004.
- Milsom I, Abrams P, Cardozo L, Roberts RG, Thüroff J, Wein AJ. How widespread are the symptoms of an overactive bladder and how are

- they managed? A population-based prevalence study. *BJU Int* 87: 760–766, 2001.
31. **Morimura K, Ohi Y, Yamamura H, Ohya S, Muraki K, Imaizumi Y.** Two-step Ca^{2+} intracellular release underlies excitation-contraction coupling in mouse urinary bladder myocytes. *Am J Physiol Cell Physiol* 290: C388–C403, 2006.
 32. **Murata H, Hotta S, Sawada E, Yamamura H, Ohya S, Kita S, Iwamoto T, Imaizumi Y.** Cellular Ca^{2+} dynamics in urinary bladder smooth muscle from transgenic mice overexpressing $\text{Na}^+/\text{Ca}^{2+}$ exchanger. *J Pharm Sci* 112: 373–377, 2010.
 33. **Neco P, Rose B, Huynh N, Zhang R, Bridge JH, Philipson KD, Goldhaber JL.** Sodium-calcium exchange is essential for effective triggering of calcium release in mouse heart. *Biophys J* 99: 755–764, 2010.
 34. **Ohi Y, Takai N, Muraki K, Watanabe M, Imaizumi Y.** Ca^{2+} -images of smooth muscle cells and endothelial cells in one confocal plane in femoral artery segments of the rat. *Jpn J Pharmacol* 86: 106–113, 2001.
 35. **Ohi Y, Yamamura H, Nagano N, Ohya S, Muraki K, Watanabe M, Imaizumi Y.** Local Ca^{2+} transients and distribution of BK channels and ryanodine receptors in smooth muscle cells of guinea-pig vas deferens and urinary bladder. *J Physiol* 534: 313–326, 2001.
 36. **Pulina MV, Zulian A, Berra-Romani R, Beskina O, Mazzocco-Spezia A, Baryshnikov SG, Papparella I, Hamlyn JM, Blaustein MP, Golovina VA.** Upregulation of Na^+ and Ca^{2+} transporters in arterial smooth muscle from ouabain-induced hypertensive rats. *Am J Physiol Heart Circ Physiol* 298: H263–H274, 2010.
 37. **Quednau BD, Nicoll DA, Philipson KD.** The sodium/calcium exchanger family-SLC8. *Pflügers Arch* 447: 543–548, 2004.
 38. **Quednau BD, Nicoll DA, Philipson KD.** Tissue specificity and alternative splicing of the $\text{Na}^+/\text{Ca}^{2+}$ exchanger isoforms NCX1, NCX2, and NCX3 in rat. *Am J Physiol Cell Physiol* 272: C1250–C1261, 1997.
 39. **Raina H, Ella SR, Hill MA.** Decreased activity of the smooth muscle $\text{Na}^+/\text{Ca}^{2+}$ exchanger impairs arteriolar myogenic reactivity. *J Physiol* 586: 1669–1681, 2008.
 40. **Rebolledo A, Speroni F, Raingo J, Salemme SV, Tanzi F, Munin V, Anon MC, Milesi V.** The $\text{Na}^+/\text{Ca}^{2+}$ exchanger is active and working in the reverse mode in human umbilical artery smooth muscle cells. *Biochem Biophys Res Commun* 339: 840–845, 2006.
 41. **Shigekawa M, Iwamoto T.** Cardiac $\text{Na}^+/\text{Ca}^{2+}$ exchange: molecular and pharmacological aspects. *Circ Res* 88: 864–876, 2001.
 42. **Slodzinski MK, Blaustein MP.** Physiological effects of $\text{Na}^+/\text{Ca}^{2+}$ exchanger knockdown by antisense oligodeoxynucleotides in arterial myocytes. *Am J Physiol Cell Physiol* 275: C251–C259, 1998.
 43. **Stewart WF, Van Rooyen JB, Cundiff GW, Abrams P, Herzog AR, Corey R, Hunt TL, Wein AJ.** Prevalence and burden of overactive bladder in the United States. *World J Urol* 20: 327–336, 2003.
 44. **Van Breemen C, Aaronson P, Loutzenhiser R.** Sodium-calcium interactions in mammalian smooth muscle. *Pharmacol Rev* 30: 167–208, 1978.
 45. **Wakimoto K, Kobayashi K, Kuro OM, Yao A, Iwamoto T, Yanaka N, Kita S, Nishida A, Azuma S, Toyoda Y, Omori K, Imahie H, Oka T, Kudoh S, Kohmoto O, Yazaki Y, Shigekawa M, Imai Y, Nabeshima Y, Komuro I.** Targeted disruption of $\text{Na}^+/\text{Ca}^{2+}$ exchanger gene leads to cardiomyocyte apoptosis and defects in heartbeat. *J Biol Chem* 275: 36991–36998, 2000.
 46. **Wang J, Chan TO, Zhang XQ, Gao E, Song J, Koch WJ, Feldman AM, Cheung JY.** Induced overexpression of $\text{Na}^+/\text{Ca}^{2+}$ exchanger transgene: altered myocyte contractility, $[\text{Ca}^{2+}]_i$ transients, SR Ca^{2+} contents, and action potential duration. *Am J Physiol Heart Circ Physiol* 297: H590–H601, 2009.
 47. **Watano T, Kimura J, Morita T, Nakanishi H.** A novel antagonist, No. 7943, of the $\text{Na}^+/\text{Ca}^{2+}$ exchange current in guinea-pig cardiac ventricular cells. *Br J Pharmacol* 119: 555–563, 1996.
 48. **Yamamura H, Ikeda C, Suzuki Y, Ohya S, Imaizumi Y.** Molecular assembly and dynamics of fluorescent protein-tagged single $\text{K}_{\text{Ca}}1.1$ channel in expression system and vascular smooth muscle cells. *Am J Physiol Cell Physiol* 302: C1257–C1268, 2012.
 49. **Yamamura H, Imaizumi Y.** Total internal reflection fluorescence imaging of Ca^{2+} -induced Ca^{2+} release in mouse urinary bladder smooth muscle cells. *Biochem Biophys Res Commun* 427: 54–59, 2012.
 50. **Yamamura H, Nagano N, Hirano M, Muraki K, Watanabe M, Imaizumi Y.** Activation of Ca^{2+} -dependent K^+ current by nordihydroguaiaretic acid in porcine coronary arterial smooth muscle cells. *J Pharmacol Exp Ther* 291: 140–146, 1999.
 51. **Yamanaka J, Nishimura J, Hirano K, Kanaide H.** An important role for the $\text{Na}^+/\text{Ca}^{2+}$ exchanger in the decrease in cytosolic Ca^{2+} concentration induced by isoprenaline in the porcine coronary artery. *J Physiol* 549: 553–562, 2003.
 52. **Yamashita J, Kita S, Iwamoto T, Ogata M, Takaoka M, Tazawa N, Nishikawa M, Wakimoto K, Shigekawa M, Komuro I, Matsumura Y.** Attenuation of ischemia/reperfusion-induced renal injury in mice deficient in $\text{Na}^+/\text{Ca}^{2+}$ exchanger. *J Pharmacol Exp Ther* 304: 284–293, 2003.
 53. **Yamazaki D, Tabara Y, Kita S, Hanada H, Komazaki S, Naitou D, Mishima A, Nishi M, Yamamura H, Yamamoto S, Kakizawa S, Miyachi H, Miyata T, Kawano Y, Kamide K, Ogihara T, Hata A, Umemura S, Soma M, Takahashi N, Imaizumi Y, Miki T, Iwamoto T, Takeshima H.** TRIC-A channels in vascular smooth muscle contribute to blood pressure maintenance. *Cell Metab* 14: 231–241, 2011.
 54. **Zhang J, Ren C, Chen L, Navedo MF, Antos LK, Kinsey SP, Iwamoto T, Philipson KD, Kotlikoff MI, Santana LF, Wier WG, Matteson DR, Blaustein MP.** Knockout of $\text{Na}^+/\text{Ca}^{2+}$ exchanger in smooth muscle attenuates vasoconstriction and L-type Ca^{2+} channel current and lowers blood pressure. *Am J Physiol Heart Circ Physiol* 298: H1472–H1483, 2010.
 55. **Zhang S, Dong H, Rubin LJ, Yuan JX.** Upregulation of $\text{Na}^+/\text{Ca}^{2+}$ exchanger contributes to the enhanced Ca^{2+} entry in pulmonary artery smooth muscle cells from patients with idiopathic pulmonary arterial hypertension. *Am J Physiol Cell Physiol* 292: C2297–C2305, 2007.
 56. **Zhang S, Yuan JX, Barrett KE, Dong H.** Role of $\text{Na}^+/\text{Ca}^{2+}$ exchange in regulating cytosolic Ca^{2+} in cultured human pulmonary artery smooth muscle cells. *Am J Physiol Cell Physiol* 288: C245–C252, 2005.